Semi-Inclusive Deep-Inelastic Scattering at NNLO in QCD

Sven-Olaf Moch

Universität Hamburg

Universität Hamburg
DER FORSCHUNG | DER LEHRE | DER BILDUNG

erc
European Research Council
Established by the European Commission

INT Program "Precision QCD with the Electron-Ion Collider" Seattle, May 15, 2025

This talk is based on:

- *NNLO QCD corrections to unpolarized and polarized SIDIS*
  S. Goyal, R.N. Lee, S. M., V. Pathak, N. Rana and V. Ravindran
  arXiv:2412.19309

- *NNLO phase-space integrals for semi-inclusive deep-inelastic scattering*
  T. Ahmed, S. Goyal, S. M. Hasan, R.N. Lee, S. M., V. Pathak, N. Rana, A. Rapakoulias and V. Ravindran
  arXiv:2412.16509

- *NNLO QCD corrections to polarized semi-inclusive DIS*
  S. Goyal, R.N. Lee, S. M., V. Pathak, N. Rana and V. Ravindran
  arXiv:2404.09959

- *Next-to-Next-to-Leading Order QCD Corrections to Semi-Inclusive Deep-Inelastic Scattering*
  S. Goyal, S. M., V. Pathak, N. Rana and V. Ravindran
  arXiv:2312.17711

Related work:

- *Identified Hadron Production in Deeply Inelastic Neutrino-Nucleon Scattering*
  L. Bonino, T. Gehrmann, M. Löchner and K. Schönwald
  arXiv:2504.05376
- *Polarized semi-inclusive deep-inelastic scattering at NNLO in QCD*
  L. Bonino, T. Gehrmann, M. Löchner, K. Schönwald and G. Stagnitto
  arXiv:2404.08597
- *Semi-Inclusive Deep-Inelastic Scattering at Next-to-Next-to-Leading Order in QCD*
  L. Bonino, T. Gehrmann, and G. Stagnitto arXiv:2401.16281

Semi-inclusive deep-inelastic scattering

- SIDIS
  - production of identified hadrons in DIS
  - multiple hadron species: π, K, D, p, n, Λ, . .
  - probe of hadron structure in broad kinematic range

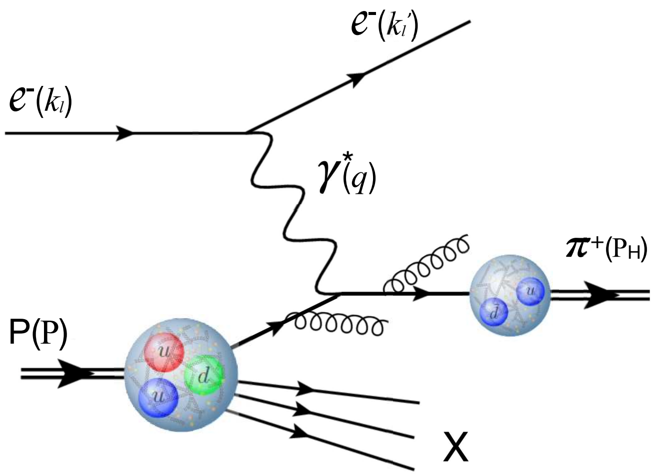

- QCD factorization at scale μ^2

$$\sigma_{\gamma H \to H'} = \sum_{ij} f_{i/H}(\mu^2) \otimes \hat{\sigma}_{\gamma i \to j}\left(\alpha_s(\mu^2), Q^2, \mu^2\right) \otimes D_{H'/j}(\mu^2)$$

  - parton distribution function (PDF) $f_{i/H}(x, \mu^2)$
  - parton-to-hadron fragmentation function (FF) $D_{H'/j}(z, \mu^2)$
- Perturbative QCD
  - hard scattering cross section $\hat{\sigma}_{\gamma i \to j}\left(x, z, \alpha_s(\mu^2), Q^2, \mu^2\right)$ computed to NNLO

Once upon a time ...

- HERA: deep structure of proton at highest Q^2 and smallest x

Bright future for precision hadron physics

- Electron-Ion Collider

  A machine that will unlock the secrets of the strongest force in Nature

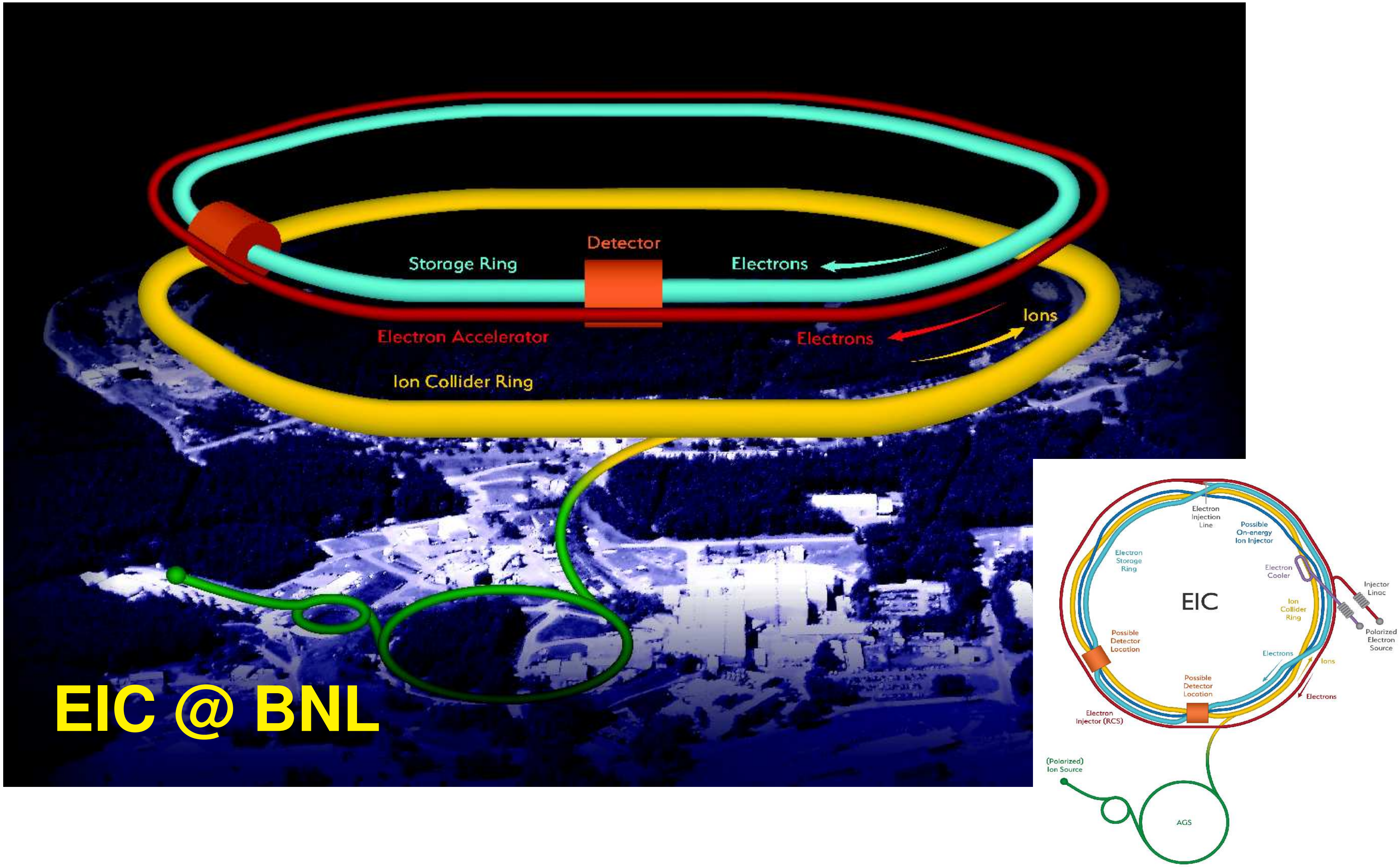

SIDIS process

- $l(k_l) + H(P) \to l(k_l') + H'(P_H) + X$
  - space-like momentum transfer $q = k_l - k_l'$ with $Q^2 = -q^2$
  - Bjorken variable $x = \frac{Q^2}{2P\cdot q}$
  - inelasticity $y = \frac{P\cdot q}{P\cdot k_l}$
  - fragmenting hadron variable $z = \frac{P\cdot P_H}{P\cdot q}$

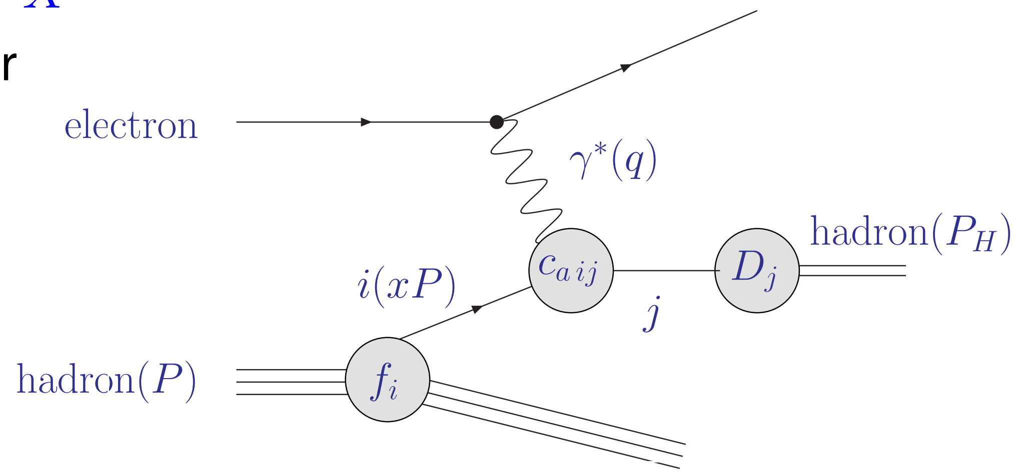

- Cross sections parametrized through structure functions
  - unpolarized SIDIS $\sigma = \frac{1}{4}\sum_{s_l,S,s_l',S_H} \sigma_{s_l,S}^{s_l',S_H}$

$$\frac{d^3\sigma}{dxdydz} = \frac{4\pi\alpha_e^2}{Q^2}\left[yF_1(x,z,Q^2) + \frac{(1-y)}{y}F_2(x,z,Q^2)\right]$$

  - polarized SIDIS $\Delta\sigma = \frac{1}{2}\sum_{s_l',S_H}\left(\sigma_{s_l=\frac{1}{2},S=\frac{1}{2}}^{s_l',S_H} - \sigma_{s_l=\frac{1}{2},S=-\frac{1}{2}}^{s_l',S_H}\right)$

$$\frac{d^3\Delta\sigma}{dxdydz} = \frac{4\pi\alpha_e^2}{Q^2}(2-y)g_1(x,z,Q^2)$$

Structure functions in perturbative QCD

- QCD factorization for structure function F_2 (up to order $\mathcal{O}(1/Q^2)$)

$$x^{-1} F_2(x,z,Q^2) \; = \; \sum_{ij} \int_x^1 \frac{dx'}{x'} \int_z^1 \frac{dz'}{z'} \, f_{i/H}(x',\mu^2) \, C_{2,ij}\left(\frac{x}{x'}, \frac{z}{z'}, \alpha_s(\mu^2), \frac{\mu^2}{Q^2}\right) D_{H'/j}(z',\mu^2)$$

  - coefficient functions $C_{a,ij} = \alpha_s^n \left(c^{(0)}_{a,ij} + \alpha_s c^{(1)}_{a,ij} + \alpha_s^2 c^{(2)}_{a,ij} + \ldots \right)$
- Analogous for $g_1(x,z,Q^2)$ with polarized PDFs $\Delta f_{i/H}(x',\mu^2)$ and coefficient functions $\Delta C_{1,ij}$

Parton evolution

$$\frac{d}{d \ln \mu^2} f_{i/H}(x,\mu^2) \quad = \quad \sum_j \left[P_{ij}(\alpha_s(\mu^2)) \otimes f_{j/H}(\mu^2) \right](x)$$

- Splitting functions $P_{ij} = \alpha_s P^{(0)}_{ij} + \alpha_s^2 P^{(1)}_{ij} + \alpha_s^3 P^{(2)}_{ij} + \alpha_s^4 P^{(3)}_{ij} + \ldots$
  - space-like splitting functions for PDFs $f_{i/H}(x,\mu^2)$
  - time-like splitting functions for FFs $D_{H'/j}(z,\mu^2)$

Coefficient functions (1)

- Leading order
- Born process $q(\bar{q}) + \gamma^* \to q(\bar{q})$
- $\mathcal{C}^{(0)}_{2,qq}(x', z') = \delta(1 - x')\, \delta(1 - z')$

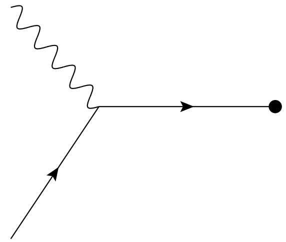

- Next-to-leading order
- Real and virtual processes

$$
\begin{aligned}
q(\bar{q}) + \gamma^* &\quad\to\quad q(\bar{q}) + \text{one loop} \\
q(\bar{q}) + \gamma^* &\quad\to\quad q(\bar{q}) + g \\
g + \gamma^* &\quad\to\quad q + \bar{q}
\end{aligned}
$$

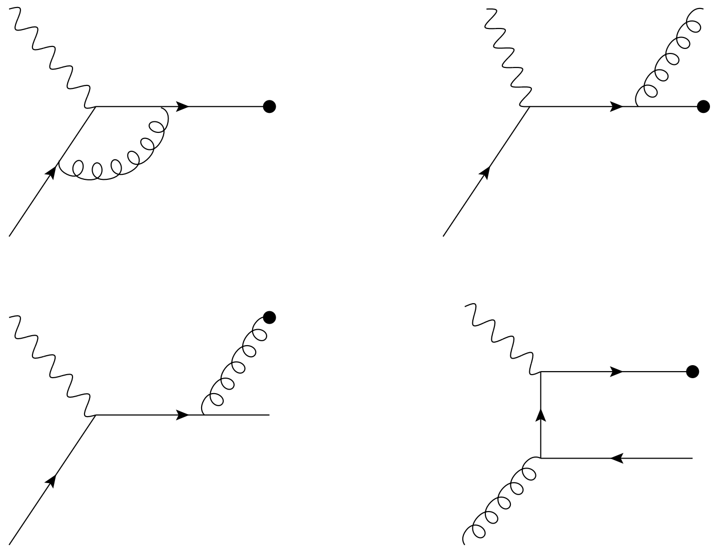

- $\mathcal{C}^{(1)}_{a,ij}(x', z')$ known since long time
  Altarelli, Ellis, Martinelli, Pi '79; de Florian, Stratmann, Vogelsang '97

Coefficient functions (2)

$$\mathcal{C}^{(2)}_{a,ij}(x',z') \sim \mathcal{P}^{\mu\nu}_a \int \mathsf{dPS}_{X+j}\, \overline{\Sigma} |M_{ij}|^2_{\mu\nu}\, \delta\Big(z' - \frac{p_i \cdot p_j}{p_i \cdot q}\Big)$$

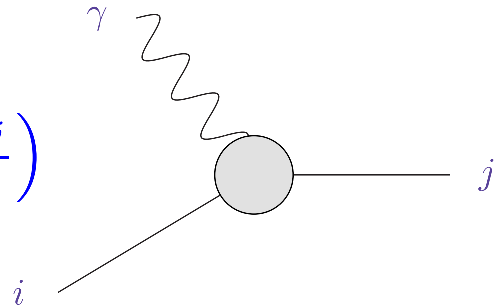

- Squared (projected) matrix elements
  - Feynman diagram with **Qgraf** Nogueira '91
  - symbolic manipulation with **Form**

    Vermaseren '00; Kuipers, Ueda, Vermaseren, Vollinga '12
  - UV and IR regularizazion in $D = 4 - 2\varepsilon$ dimensions
  - phase space integrals with kinematical constraint
- Reverse Unitarity method (Cutkosky rule)
  - phase-space integrals mapped to loop integrals

$$(2\pi i)\delta(p^2) \quad = \quad \frac{1}{p^2 + i\epsilon} + \text{cc.}$$

- Standard reduction with integration-by-parts to master integrals

Coefficient functions (3)

- Next-to-next-to-leading order
- Double-real, real-virtual and virtual processes

$$
\begin{aligned}
q(\bar{q}) + \gamma^* &\rightarrow q(\bar{q}) + \text{two loops} \\
q(\bar{q}) + \gamma^* &\rightarrow q(\bar{q}) + g + \text{one loop} \\
g + \gamma^* &\rightarrow q + \bar{q} + \text{one loop} \\
q(\bar{q}) + \gamma^* &\rightarrow q(\bar{q}) + g + g \\
g + \gamma^* &\rightarrow g + q + \bar{q} \\
q(\bar{q}) + \gamma^* &\rightarrow q(\bar{q}) + q' + \bar{q}' \\
q(\bar{q}) + \gamma^* &\rightarrow q(\bar{q}) + q + \bar{q}
\end{aligned}
$$

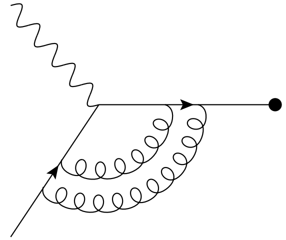

VV

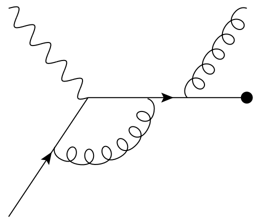

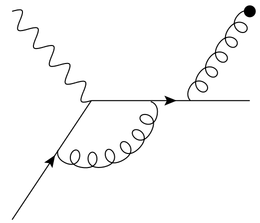

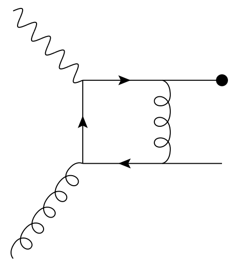

RV

- VV contributions: massless two-loop form factor

Hamberg, van Neerven, Matsuura '88

- RV contributions with box integrals $\sim \; {}_2F_1\left(-\epsilon, -\epsilon, 1-\epsilon, f(x', z')\right)$
  - care needed for analyticity in the physical domain of x', z'

Coefficient functions (4)

- Double-real emissions
- RR requires
  three body phase space integrals
- RR master integrals, functions of x', z'

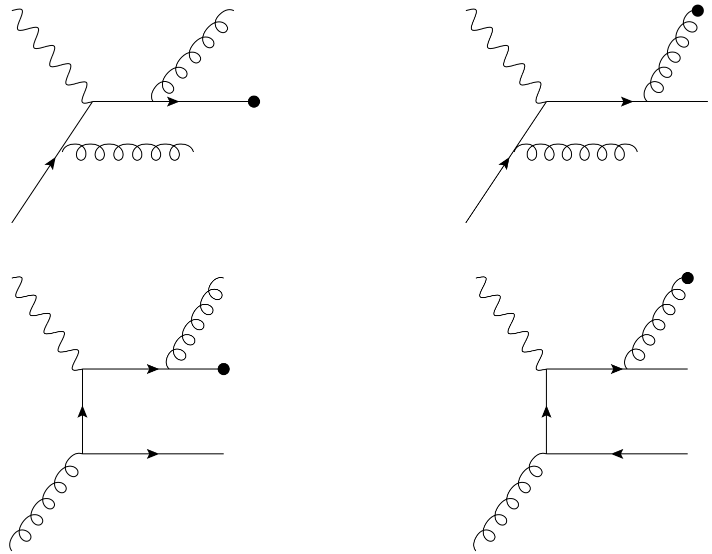

RR

Method 1

- Differential equations in x', z'
  - 20 MIs from integration-by-parts relations
  - boundary conditions by integration over z' from inclusive RR integrals (DIS coefficient functions)
- Additional relations between MIs observed from analytic solutions
  - $j_7 = j_{16}$ and $j_9 = f(j_1, j_2, j_5, j_8)$
  - not obvious from integration-by-parts relations

Coefficient functions (5)

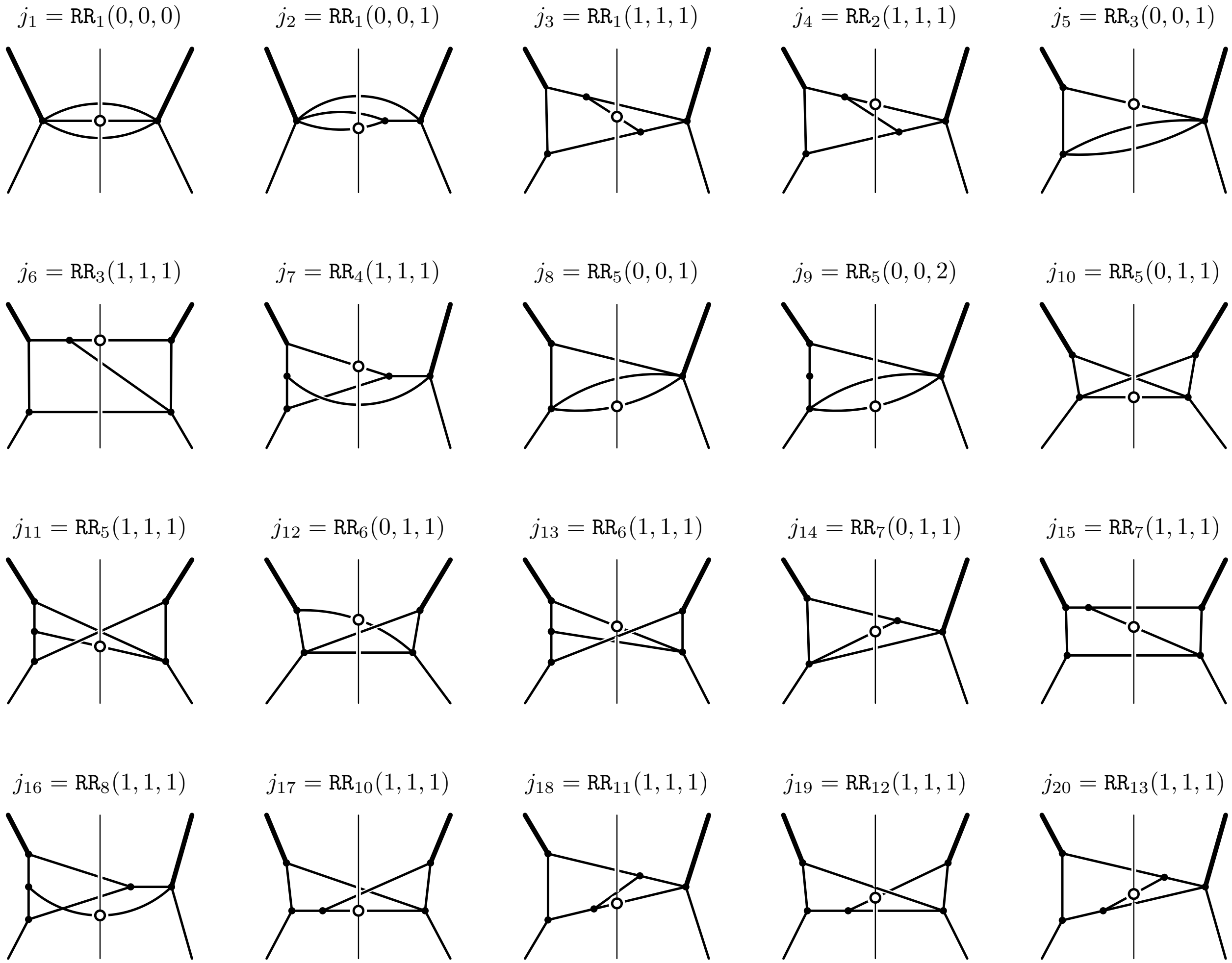

- MIs of families $\mathrm{RR}_1, \ldots, \mathrm{RR}_{13}$
  - cut lines denote cut massless propagators,
  - circle marks propagator of identified parton

Coefficient functions (6)

Method 2

- Radial-angular decomposition
  - angular integration with Mellin-Barnes method Somogyi'11
  - collinear singularities arise from angular integration
  - one-fold radial integrals $\int dz\, f(z)$ over classical polylogarithms
  - soft divergences originate from integration over z

Soft and collinear singularities

- RR phase-space integrals in $D = 4 - 2\varepsilon$

$$(1-x')^{-1-a\varepsilon}(1-z')^{-1-b\varepsilon} f(x', z', \varepsilon)$$

  - regular functions $f(x', z', \varepsilon)$ in threshold limits $x' \to 1$ and/or $z' \to 1$
- IR divergences can be isolated ($w = x', z'$) with 'plus'-distributions

$$(1-w)^{-1+n\varepsilon} = \frac{1}{n\varepsilon}\delta(1-w) + \sum_{k=0}^{\infty} \frac{(n\varepsilon)^k}{k!} \left[\frac{\log^k(1-w)}{(1-w)}\right]_+$$

Coefficient functions (7)

Threshold resummation

- Coefficient functions $\mathcal{C}^{(n)}_{a,ij}(x', z') \sim \alpha_s^n \left[\frac{\log^k(1-w)}{(1-w)}\right]_+$
  - threshold logarithms in $w = x', z'$ and $k \leq 2n - 1$
- Prediction of threshold enhanced logarithms from resummation for SIDIS in Mellin variables $(x' \rightarrow) N$ and $(z' \rightarrow) M$
  - bears much resemblance with Drell-Yan rapidity distribution $z = Q^2/\hat{s} \rightarrow N$ and $\sqrt{z}\exp(\pm y) \rightarrow M$
- Useful approach to derive approximations at higher orders

  Abele, de Florian, Vogelsang '21; '22
  - approximate NNLO and N^{3}LO QCD corrections
  - threshold resummation at N^{3}LL accuracy

Check

- Full agreement of exact computation with NNLO SV terms

Splitting functions at large x

The large x-limit: $x \to 1$

- Structure of diagonal splitting functions $P_{\rm ii}$ (for $\rm i = q, g$) at large x

$$P_{ii}^{(n-1)}(x) \;=\; \frac{A_n^{\rm i}}{(1-x)_+} + B_n^{\rm i}\,\delta(1-x) + \dots$$

- Cusp anomalous dimension $A_n^{\rm i}$
  - known from $1/\epsilon^2$-poles of QCD form factor
- Four loop results in QCD

Large-n_c (Henn, Lee, Smirnov, Smirnov, Steinhauser '16; S. M., Ruijl, Ueda, Vermaseren, Vogt '17); n_f (Grozin '18; Henn, Peraro, Stahlhofen, Wasser '19); n_f^2 (Davies, Ruijl, Ueda, Vermaseren, Vogt '16; Lee, Smirnov, Smirnov, Steinhauser '17); n_f^3 (Gracey '94; Beneke, Braun, '95);
quartic colour (Lee, Smirnov, Smirnov, Steinhauser '19; Henn, Korchemsky, Mistlberger '19)

- Virtual anomalous dimension $B_n^{\rm i}$
  - parts related to $1/\epsilon$-poles of QCD form factor

Quark virtual anomalous dimension

- Four loop result (up to one unknown $b^{q}_{4,FA}$) Kniehl, S.M., Velizhanin, Vogt '25

$$
\begin{aligned}
B_4^{q} \quad =\quad & \\
& C_F^4\left(\frac{4873}{24} - 450\zeta_2 - \frac{684}{5}\zeta_2^2 - \frac{16888}{35}\zeta_2^3 + 2004\zeta_3 - 120\zeta_3\zeta_2 + \frac{128}{5}\zeta_3\zeta_2^2 - 1152\zeta_3^2 - 2520\zeta_5 - 384\zeta_5\zeta_2 + 5880\zeta_7\right) \\
& + C_F C_A^3\left(-\frac{371201}{648} - \frac{1}{24}b^{q}_{4,FA} + \frac{4582}{3}\zeta_2 - \frac{22388}{135}\zeta_2^2 + \frac{48368}{315}\zeta_2^3 - \frac{153670}{81}\zeta_3 + \frac{472}{3}\zeta_3\zeta_2 + \frac{16}{5}\zeta_3\zeta_2^2 + 528\zeta_3^2\right. \\
& \left. + \frac{11372}{9}\zeta_5 + 504\zeta_5\zeta_2 - 2870\zeta_7\right) + C_F^2 C_A^2\left(\frac{29639}{36} - \frac{46771}{27}\zeta_2 - \frac{24340}{27}\zeta_2^2 - \frac{21988}{35}\zeta_2^3 + \frac{129662}{27}\zeta_3 + \frac{2096}{9}\zeta_3\zeta_2\right. \\
& \left. - \frac{64}{5}\zeta_3\zeta_2^2 - \frac{7102}{3}\zeta_3^2 + \frac{5354}{9}\zeta_5 - 2104\zeta_5\zeta_2 + 8610\zeta_7\right) + C_F^3 C_A\left(-\frac{2085}{4} + 1167\zeta_2 + \frac{4334}{5}\zeta_2^2 + \frac{317188}{315}\zeta_2^3\right. \\
& \left. - 3260\zeta_3 - \frac{1988}{3}\zeta_3\zeta_2 + \frac{256}{5}\zeta_3\zeta_2^2 + 3220\zeta_3^2 - 976\zeta_5 + 2064\zeta_5\zeta_2 - 10920\zeta_7\right) + \frac{d_F^{abcd}d_A^{abcd}}{n_F}\left(b^{q}_{4,FA}\right) \\
& + n_f C_F^3\left(32 + 162\zeta_2 - \frac{408}{5}\zeta_2^2 - \frac{51472}{315}\zeta_2^3 - 308\zeta_3 - \frac{256}{3}\zeta_3\zeta_2 + 224\zeta_3^2 + 912\zeta_5\right) \\
& + n_f C_F^2 C_A\left(-\frac{7751}{54} - \frac{3892}{27}\zeta_2 + \frac{55708}{135}\zeta_2^2 + \frac{2808}{35}\zeta_2^3 - \frac{15400}{27}\zeta_3 + \frac{2672}{9}\zeta_3\zeta_2 - \frac{1232}{3}\zeta_3^2 - \frac{7432}{9}\zeta_5\right) \\
& + n_f C_F C_A^2\left(\frac{20027}{108} - \frac{41092}{81}\zeta_2 + \frac{2468}{45}\zeta_2^2 - \frac{4472}{135}\zeta_2^3 + \frac{9554}{27}\zeta_3 - \frac{580}{3}\zeta_3\zeta_2 + \frac{416}{3}\zeta_3^2 + \frac{1130}{9}\zeta_5\right) \\
& + n_f \frac{d_F^{abcd}d_F^{abcd}}{n_F}\left(-192 + \frac{1888}{3}\zeta_2 - \frac{704}{15}\zeta_2^2 + \frac{2048}{45}\zeta_2^3 - \frac{992}{3}\zeta_3 + 64\zeta_3\zeta_2 + 256\zeta_3^2 - 1120\zeta_5\right) \\
& + n_f^2 C_F^2\left(-\frac{188}{27} + \frac{1244}{27}\zeta_2 - \frac{4208}{135}\zeta_2^2 + \frac{56}{27}\zeta_3 - \frac{160}{9}\zeta_3\zeta_2 + \frac{368}{9}\zeta_5\right) + n_f^2 C_F C_A\left(-\frac{193}{54} + \frac{3170}{81}\zeta_2 - \frac{32}{9}\zeta_2^2\right. \\
& \left. - \frac{320}{9}\zeta_3 + \frac{80}{3}\zeta_3\zeta_2 - \frac{88}{9}\zeta_5\right) + n_f^3 C_F\left(-\frac{131}{81} + \frac{32}{81}\zeta_2 - \frac{64}{135}\zeta_2^2 + \frac{304}{81}\zeta_3\right)
\end{aligned}
$$

Quark form factor in QCD

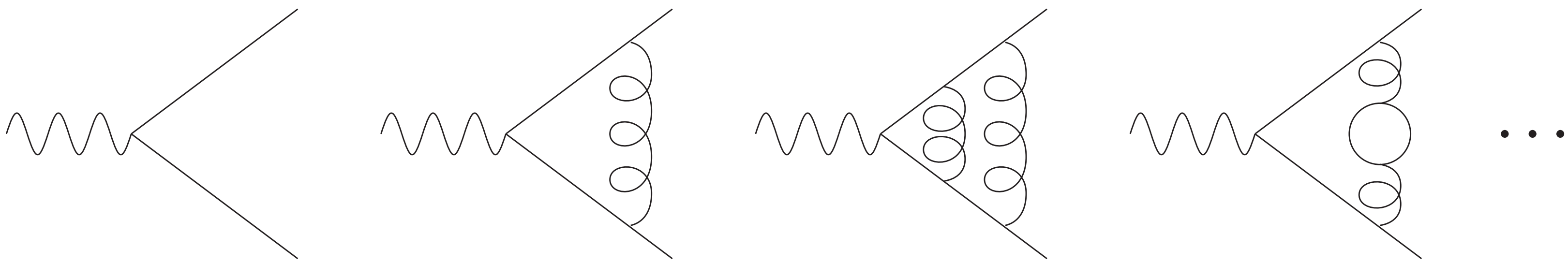

- QCD corrections to vertex $\gamma^* q\bar{q}$, i.e. $\Gamma_\mu \; = \; \mathrm{i}e_{\mathrm{q}} \left(\bar{u}\,\gamma_\mu\,u\right) \mathcal{F}_{\mathrm{q}}(Q^2, \alpha_{\mathrm{s}})$
  - gauge invariant quantity
  - infrared divergent (dimesional regularization $D = 4 - 2\epsilon$)
- Form factor $\mathcal{F}(Q^2, \alpha_s)$ exponentiates Collins '80; Sen '81; Korchemsky '88; Magnea, Sterman '90; Contopanagos, Laenen, Sterman '97; Magnea '00 (long history)

$$Q^2 \frac{\partial}{\partial Q^2} \ln \mathcal{F}\left(Q^2, \alpha_s, \epsilon\right) \; = \; \frac{1}{2}\, K(\alpha_s, \epsilon) + \frac{1}{2}\, G\left(\frac{Q^2}{\mu^2}, \alpha_s, \epsilon\right) \, .$$

- Renormalization group equations for functions G and K
  - all Q^2-scale dependence in G (finite in ϵ)
  - pure counter term function K (contains poles in $\frac{1}{\epsilon}$)
- Cusp anomalous dimension A governs evolution for G and K

Result

- Result up to four loops in terms of expansion coefficients of A and G

$$
\begin{aligned}
\mathcal{F}_1 &= -\frac{1}{2}\frac{1}{\epsilon^2}A_1 - \frac{1}{2}\frac{1}{\epsilon}G_1 \\
\mathcal{F}_2 &= \frac{1}{8}\frac{1}{\epsilon^4}A_1^2 + \frac{1}{8}\frac{1}{\epsilon^3}A_1(2G_1 - \beta_0) + \frac{1}{8}\frac{1}{\epsilon^2}(G_1^2 - A_2 - 2\beta_0 G_1) - \frac{1}{4}\frac{1}{\epsilon}G_2 \\
\mathcal{F}_3 &= -\frac{1}{48}\frac{1}{\epsilon^6}A_1^3 - \frac{1}{16}\frac{1}{\epsilon^5}A_1^2(G_1 - \beta_0) - \frac{1}{144}\frac{1}{\epsilon^4}A_1(9G_1^2 - 9A_2 - 27\beta_0 G_1 + 8\beta_0^2) \\
&\quad - \frac{1}{144}\frac{1}{\epsilon^3}(3G_1^3 - 9A_2G_1 - 18A_1G_2 + 4\beta_1 A_1 - 18\beta_0 G_1^2 + 16\beta_0 A_2 + 24\beta_0^2 G_1) \\
&\quad + \frac{1}{72}\frac{1}{\epsilon^2}(9G_1G_2 - 4A_3 - 6\beta_1 G_1 - 24\beta_0 G_2) - \frac{1}{6}\frac{1}{\epsilon}G_3 \\
\mathcal{F}_4 &= \ldots
\end{aligned}
$$

- Expansion in terms of bare coupling $a_s^{\rm b} = \alpha_s^{\rm b}/(4\pi)$

$$
\mathcal{F}\left(Q^2, \alpha_s^{\rm b}\right) = 1 + \sum_{l=1} \left(a_s^{\rm b}\right)^l \left(\frac{Q^2}{\mu^2}\right)^{-l\epsilon} \mathcal{F}_l
$$

Result

- Result up to four loops in terms of expansion coefficients of A and G

$$
\begin{aligned}
\mathcal{F}_1 &= -\frac{1}{2}\frac{1}{\epsilon^2}A_1 - \frac{1}{2}\frac{1}{\epsilon}G_1 \\
\mathcal{F}_2 &= \frac{1}{8}\frac{1}{\epsilon^4}A_1^2 + \frac{1}{8}\frac{1}{\epsilon^3}A_1(2G_1 - \beta_0) + \frac{1}{8}\frac{1}{\epsilon^2}(G_1^2 - A_2 - 2\beta_0 G_1) - \frac{1}{4}\frac{1}{\epsilon}G_2 \\
\mathcal{F}_3 &= -\frac{1}{48}\frac{1}{\epsilon^6}A_1^3 - \frac{1}{16}\frac{1}{\epsilon^5}A_1^2(G_1 - \beta_0) - \frac{1}{144}\frac{1}{\epsilon^4}A_1(9G_1^2 - 9A_2 - 27\beta_0 G_1 + 8\beta_0^2) \\
&\quad - \frac{1}{144}\frac{1}{\epsilon^3}(3G_1^3 - 9A_2G_1 - 18A_1G_2 + 4\beta_1 A_1 - 18\beta_0 G_1^2 + 16\beta_0 A_2 + 24\beta_0^2 G_1) \\
&\quad + \frac{1}{72}\frac{1}{\epsilon^2}(9G_1G_2 - 4A_3 - 6\beta_1 G_1 - 24\beta_0 G_2) - \frac{1}{6}\frac{1}{\epsilon}G_3 \\
\mathcal{F}_4 &= \ldots
\end{aligned}
$$

$\mathcal{F}_2$: Hamberg, van Neerven, Matsuura ‘88; Harlander ‘00; Gehrmann, Huber, Maitre ’05; S.M. Vermaseren, Vogt ’05

$\mathcal{F}_3$: S.M. Vermaseren, Vogt ’05; Baikov, Chetyrkin, Smirnov, Smirnov, Steinhauser ‘09; Gehrmann, Glover, Huber, Ikizlerli, Studerus ‘10

$\mathcal{F}_4$: Henn, Smirnov, Smirnov, Steinhauser, Lee ‘16; Lee, Smirnov, Smirnov, Steinhauser ‘17 & ‘19; von Manteuffel, Schabinger ‘19

Universality of subleading infrared poles

- Universal subleading infrared poles in function G Dixon, Magnea, Sterman '08
- Coefficients G_n at n-loops are composed of:
  - twice the $\delta(1-x)$ part B^{q} in parton splitting function
  - single-logarithmic anomalous dimension of *eikonal* form factor
  - terms associated with QCD beta function

$$
\begin{aligned}
G_1 &= 2B_1^{\mathrm{q}} + f_1^{\mathrm{q}} + \varepsilon f_{01}^{\mathrm{q}}\,, \\
G_2 &= 2B_2^{\mathrm{q}} + (f_2^{\mathrm{q}} + \beta_0 f_{01}^{\mathrm{q}}) + \varepsilon f_{02}^{\mathrm{q}}\,, \\
G_3 &= 2B_3^{\mathrm{q}} + (f_3^{\mathrm{q}} + \beta_1 f_{01}^{\mathrm{q}} + \beta_0 f_{02}^{\mathrm{q}}) + \varepsilon f_{03}^{\mathrm{q}}\,, \\
G_4 &= 2B_4^{\mathrm{q}} + (f_4^{\mathrm{q}} + \beta_2 f_{01}^{\mathrm{q}} + \beta_1 f_{02}^{\mathrm{q}} + \beta_0 f_{03}^{\mathrm{q}}) + \varepsilon f_{04}^{\mathrm{q}}
\end{aligned}
$$

- f-function shares maximal non-Abelian property and (generalized) Casimir scaling with cusp anomalous dimensions

$$
\begin{aligned}
f_1^{\mathrm{q}} &= 0\,, \\
f_2^{\mathrm{q}} &= C_F\left\{C_A\left(\frac{808}{27} - \frac{22}{3}\zeta_2 - 28\zeta_3\right) + n_f\left(-\frac{112}{27} + \frac{4}{3}\zeta_2\right)\right\}, \\
f_3^{\mathrm{q}} &= \dots
\end{aligned}
$$

Eikonal anomalous dimension

- Four loop result (same unknown $b^{\mathrm{q}}_{4,FA}$ as in B^{q}_4)

Kniehl, S.M., Velizhanin, Vogt '25

$$
\begin{aligned}
f^{\mathrm{q}}_4 \;=\;& C_F C_A^3 \Big(\frac{9311591}{6561} + \frac{1}{12}\, b^{\mathrm{q}}_{4,FA} - \frac{1164703}{729}\zeta_2 + \frac{231518}{135}\zeta_2^2 - \frac{173888}{315}\zeta_2^3 - \frac{829204}{243}\zeta_3 + \frac{12568}{9}\zeta_3\zeta_2 \\
& - \frac{4228}{15}\zeta_3\zeta_2^2 - \frac{4378}{9}\zeta_3^2 + \frac{106934}{27}\zeta_5 - \frac{1376}{3}\zeta_5\zeta_2 - \frac{11071}{6}\zeta_7 \Big) + \frac{d_F^{abcd} d_A^{abcd}}{n_F} \Big(192 - 2\, b^{\mathrm{q}}_{4,FA} \\
& - \frac{2176}{3}\zeta_2 + \frac{224}{15}\zeta_2^2 + \frac{27808}{315}\zeta_2^3 - \frac{7808}{9}\zeta_3 - 1792\zeta_3\zeta_2 - \frac{736}{5}\zeta_3\zeta_2^2 - \frac{3344}{3}\zeta_3^2 - \frac{1840}{9}\zeta_5 \\
& + 1024\zeta_5\zeta_2 + 3484\zeta_7 \Big) + n_f C_F^3 \Big(\frac{21037}{108} - 2\zeta_2 + \frac{148}{5}\zeta_2^2 - \frac{320}{7}\zeta_2^3 + \frac{4424}{9}\zeta_3 - 80\zeta_3^2 - \frac{1600}{3}\zeta_5 \Big) \\
& + n_f C_F^2 C_A \Big(- \frac{813475}{972} + \frac{2819}{9}\zeta_2 - \frac{1976}{45}\zeta_2^2 + \frac{128}{35}\zeta_2^3 + \frac{68882}{81}\zeta_3 - 160\zeta_3\zeta_2 - 312\zeta_3^2 + \frac{1448}{9}\zeta_5 \Big) \\
& + n_f C_F C_A^2 \Big(- \frac{394109}{1944} + \frac{294539}{729}\zeta_2 - \frac{4420}{9}\zeta_2^2 + \frac{27032}{189}\zeta_2^3 - \frac{31340}{243}\zeta_3 - \frac{104}{9}\zeta_3\zeta_2 + \frac{4420}{9}\zeta_3^2 \\
& - \frac{692}{27}\zeta_5 \Big) + n_f \frac{d_F^{abcd} d_F^{abcd}}{n_F} \Big(256\zeta_2 - \frac{64}{5}\zeta_2^2 - \frac{1280}{21}\zeta_2^3 + \frac{640}{9}\zeta_3 - \frac{320}{3}\zeta_3^2 - \frac{1600}{9}\zeta_5 \Big) \\
& + n_f^2 C_F^2 \Big(\frac{16733}{486} - \frac{172}{9}\zeta_2 + \frac{128}{45}\zeta_2^2 - \frac{4568}{81}\zeta_3 + \frac{32}{3}\zeta_3\zeta_2 + \frac{304}{9}\zeta_5 \Big) + n_f^2 C_F C_A \Big(\frac{27875}{17496} - \frac{15481}{729}\zeta_2 \\
& + \frac{776}{45}\zeta_2^2 + \frac{32152}{243}\zeta_3 - \frac{224}{9}\zeta_3\zeta_2 - 112\zeta_5 \Big) + n_f^3 C_F \Big(- \frac{16160}{6561} - \frac{16}{81}\zeta_2 + \frac{256}{135}\zeta_2^2 - \frac{400}{243}\zeta_3 \Big)
\end{aligned}
$$

Results (1)

- Unpolarized non-singlet coefficient function $\mathcal{C}^{(2)}_{2,qq}$

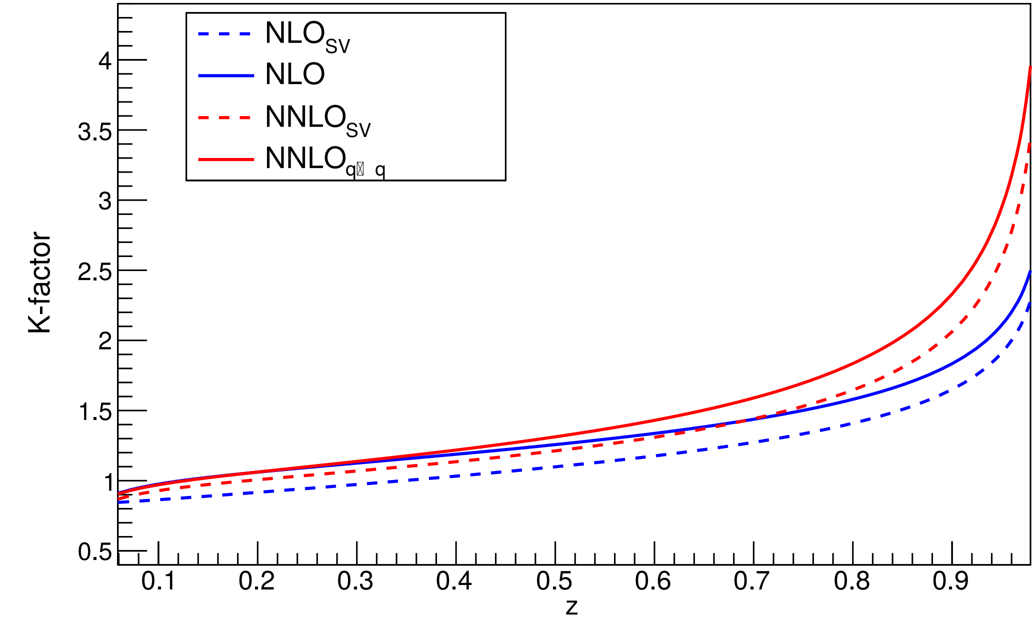

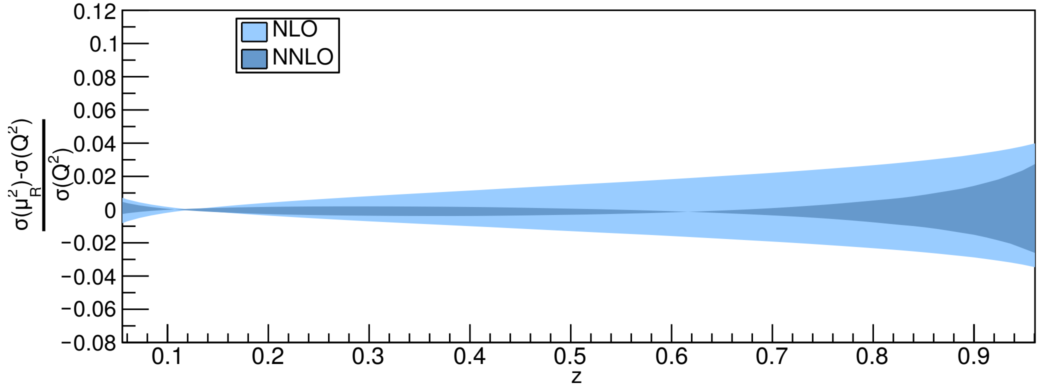

- K-factor as function of z for EIC with $\sqrt{s} = 140$ GeV
  - SV terms at NLO (blue dashed) and NNLO (red dashed)
  - full NLO (blue solid) and (non-singlet, leading color) NNLO (red solid)
- Uncertainty from renormalization scale variation $\mu_R^2 \in [Q^2/2, 2Q^2]$

Polarized SIDIS

- Polarized coefficient functions
  - appearance of γ_5 in vertex and spin projections
  - use Larin scheme $\gamma_5 \gamma_\mu = \frac{i}{6} \epsilon_{\mu\nu\rho\sigma} \gamma^\nu \gamma^\rho \gamma^\sigma$ Larin '93
- Structure function in Larin scheme

$$g_1(x,z) = \sum_{i,j} \Delta f_i{}^L(\mu_F^2) \otimes_{x'} \Delta \mathcal{C}_{1,ij}{}^L(\mu_F^2) \otimes_{z'} D_j(\mu_F^2)$$

- Scheme transformation (finite) from Larin to $\overline{\text{MS}}$ scheme
  - PDFs

$$\Delta f_k(\mu_F^2) = Z_{ki}(\mu_F^2) \otimes \Delta f_i{}^L(\mu_F^2)$$

  - coefficient functions

$$\Delta \mathcal{C}_{1,ij}(\mu_F^2) = (Z^{-1}(\mu_F^2))_{ik} \otimes \Delta \mathcal{C}_{1,kj}{}^L(\mu_F^2)$$

- Z_{ki} known to NNLO Matiounine, Smith, van Neerven '98

Results (2)

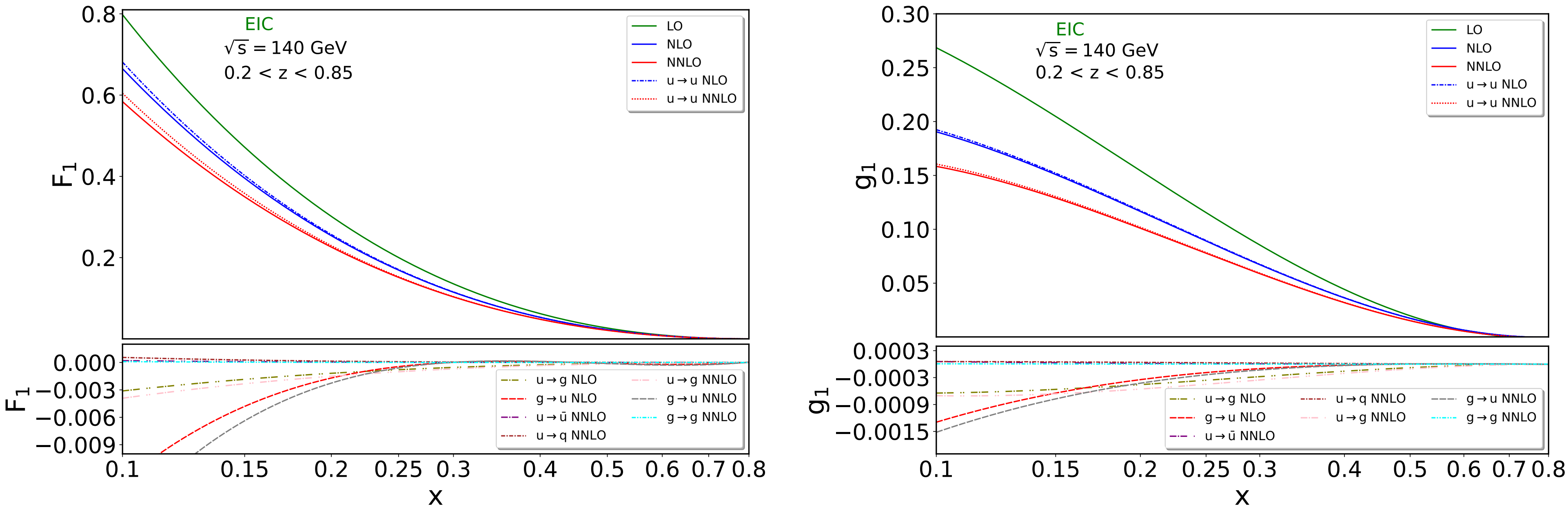

- Structure functions F_1 (left) and g_1 (right) as function of x
  - EIC at $\sqrt{s} = 140$ GeV
  - PDF sets NNPDF31 (F_1) and BDSSV24(N)NLO (g_1)
  - FF set NNFF10PIp
  - all partonic channels (non-singlet channel dominates)

Results (3)

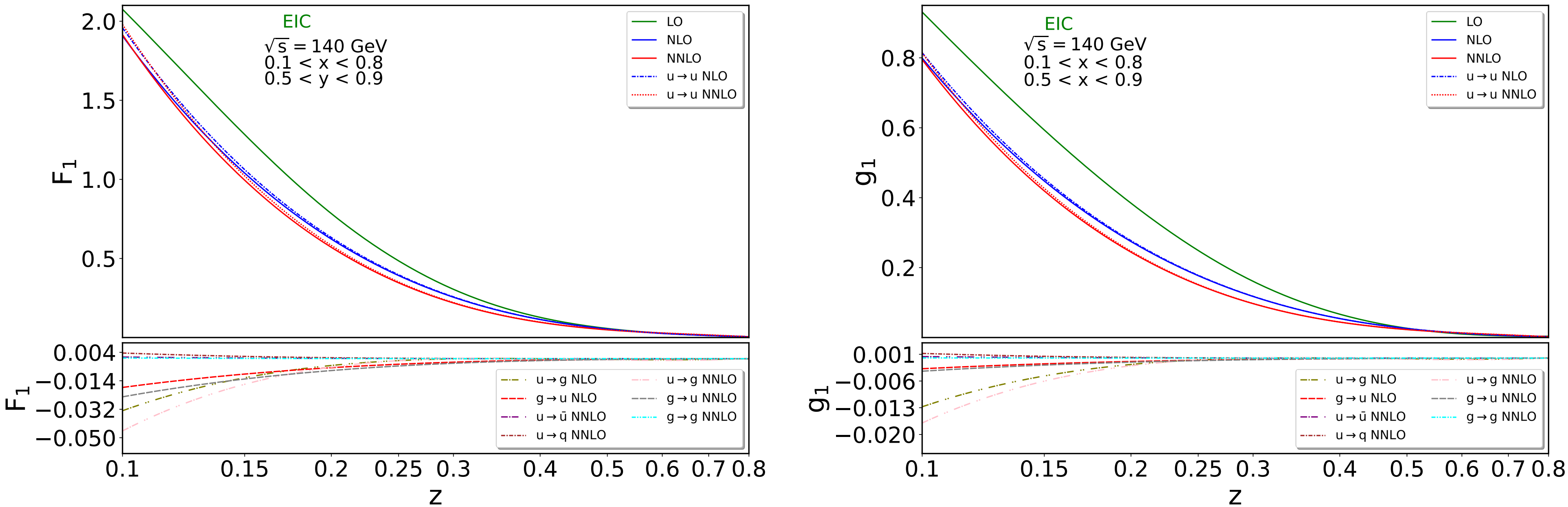

- Structure functions F_1 (left) and g_1 (right) as function of z
  - EIC at $\sqrt{s} = 140$ GeV
  - PDF sets NNPDF31 (F_1) and BDSSV24(N)NLO (g_1)
  - FF set NNFF10PIp
  - all partonic channels (non-singlet channel dominates)

Results (4)

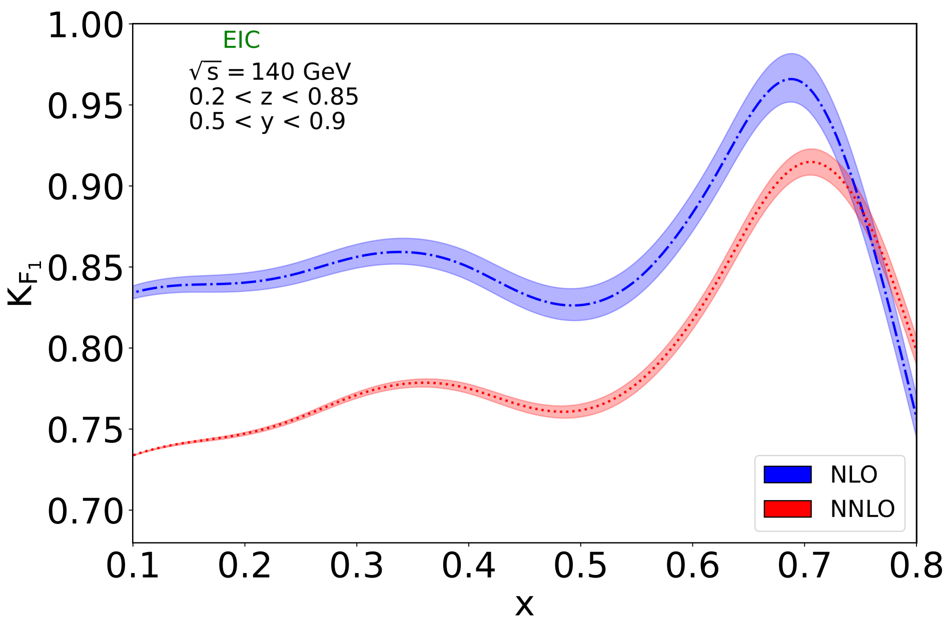

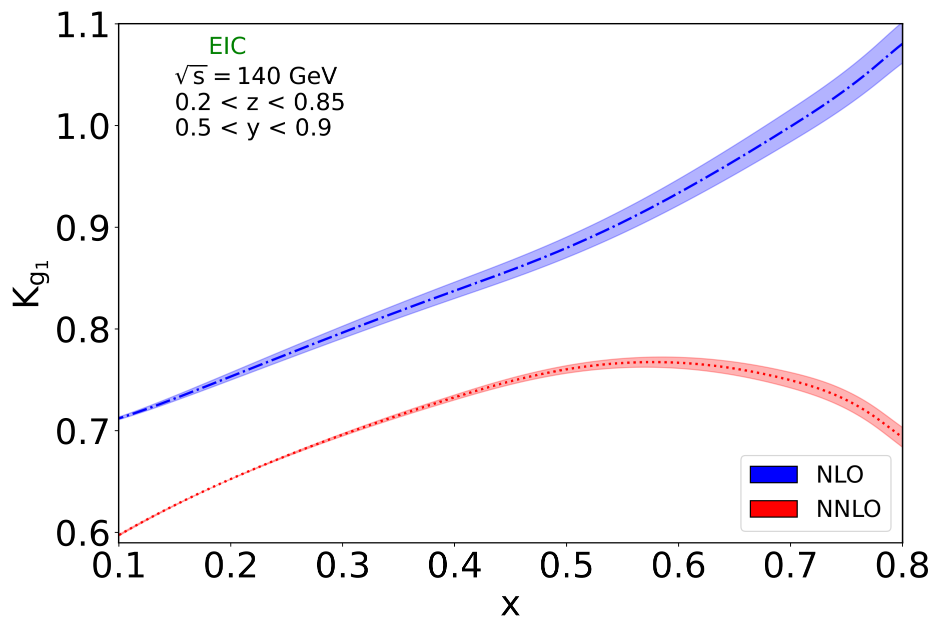

- NLO and NNLO K-factors for structure functions F_1 (left) and g_1 (right) as function of x
  - EIC at $\sqrt{s} = 140$ GeV
  - PDF sets NNPDF31 (F_1) and BDSSV24(N)NLO (g_1)
  - FF set NNFF10PIp
- Bands from variation $\mu_R \in \left[Q^2_{avg}/2, 2Q^2_{avg}\right]$; fixed $\mu_F = Q_{avg} = x y_{avg} s$

Results (5)

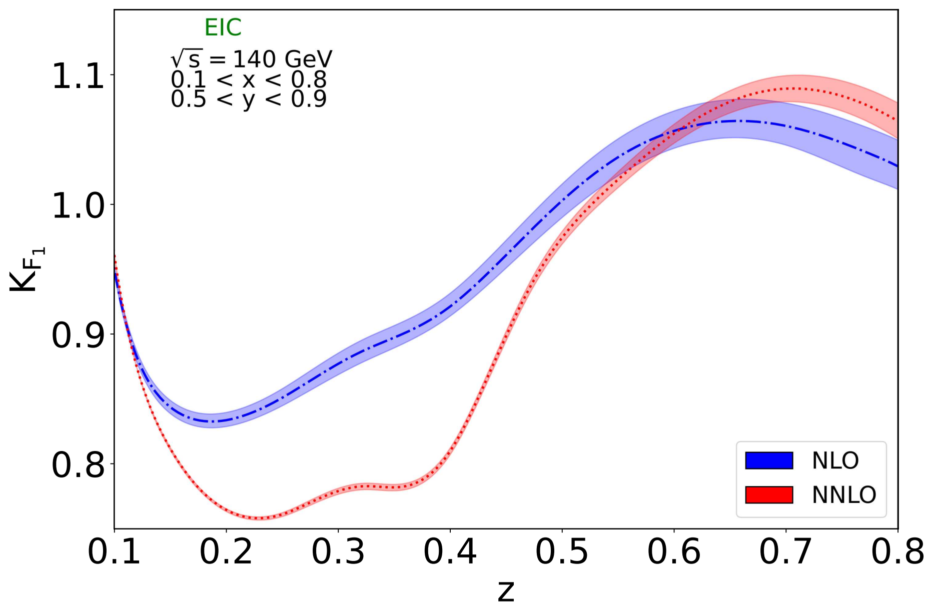

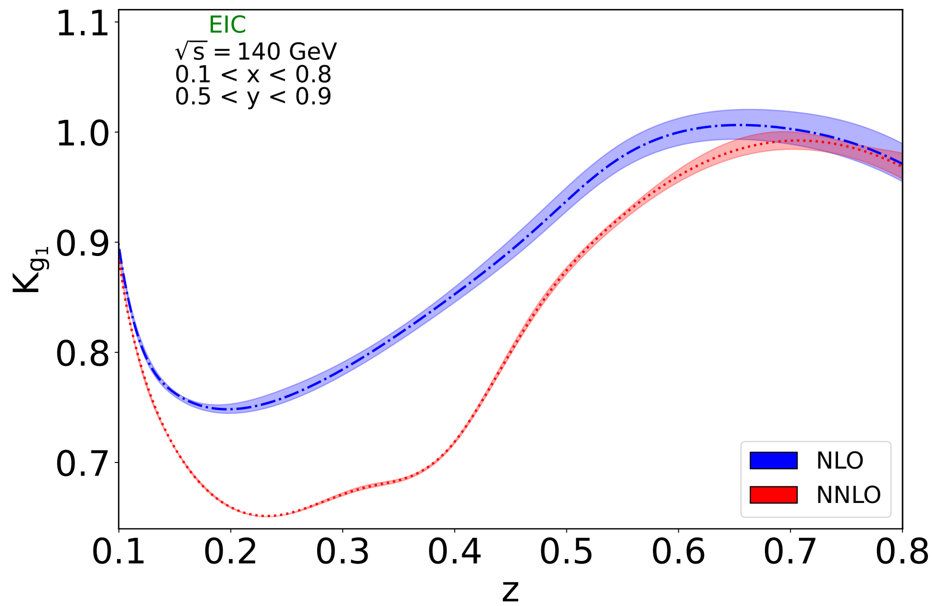

- NLO and NNLO K-factors for structure functions F_1 (left) and g_1 (right) as function of z
  - EIC at $\sqrt{s} = 140$ GeV
  - PDF sets NNPDF31 (F_1) and BDSSV24(N)NLO (g_1)
  - FF set NNFF10PIp
- Bands from variation $\mu_R \in \left[Q^2_{avg}/2, 2Q^2_{avg}\right]$; fixed $\mu_F = Q_{avg} = xy_{avg}s$

Results (6)

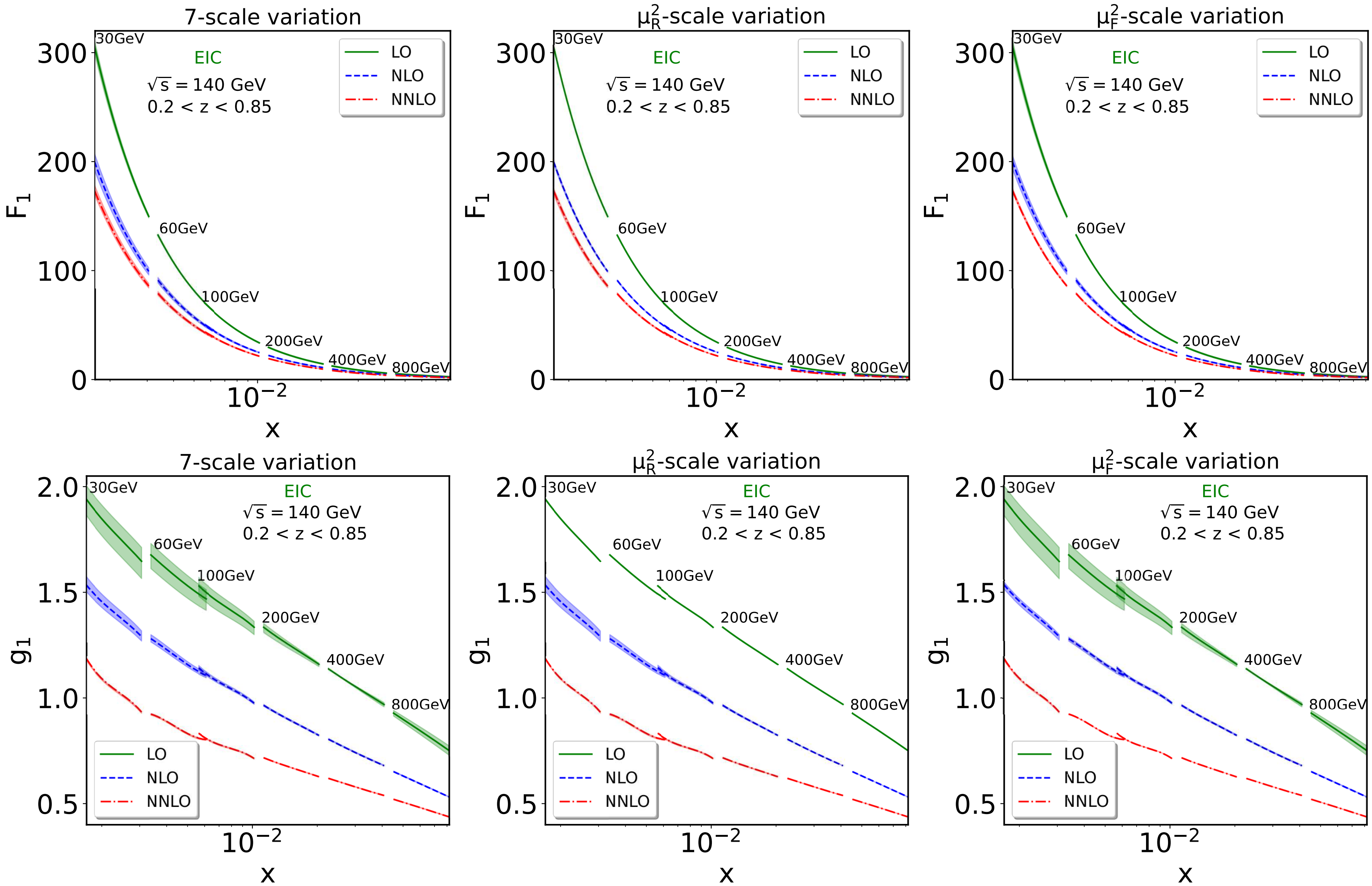

- Scale variation F_1 (upper) and g_1 (lower) as function x for six different values of Q^2; PDFs NNPDF31 (F_1); BDSSV24(N)NLO (g_1); FFs NNFF10PIp

Results (7)

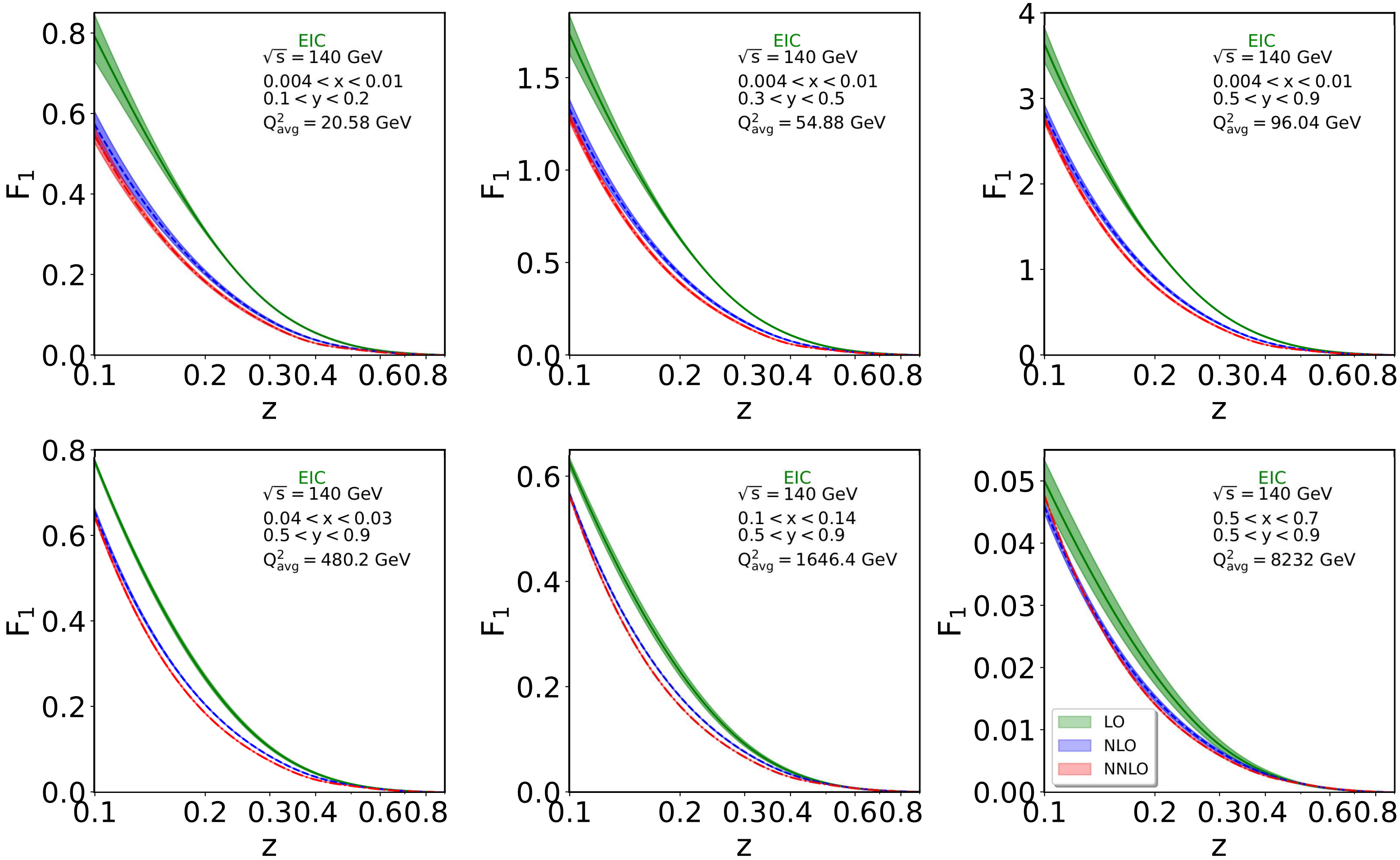

- Scale variation of F_1 as function x for six different values of Q^2 (NNPDF31 PDFs; NNFF10PIp FFs)

Results (8)

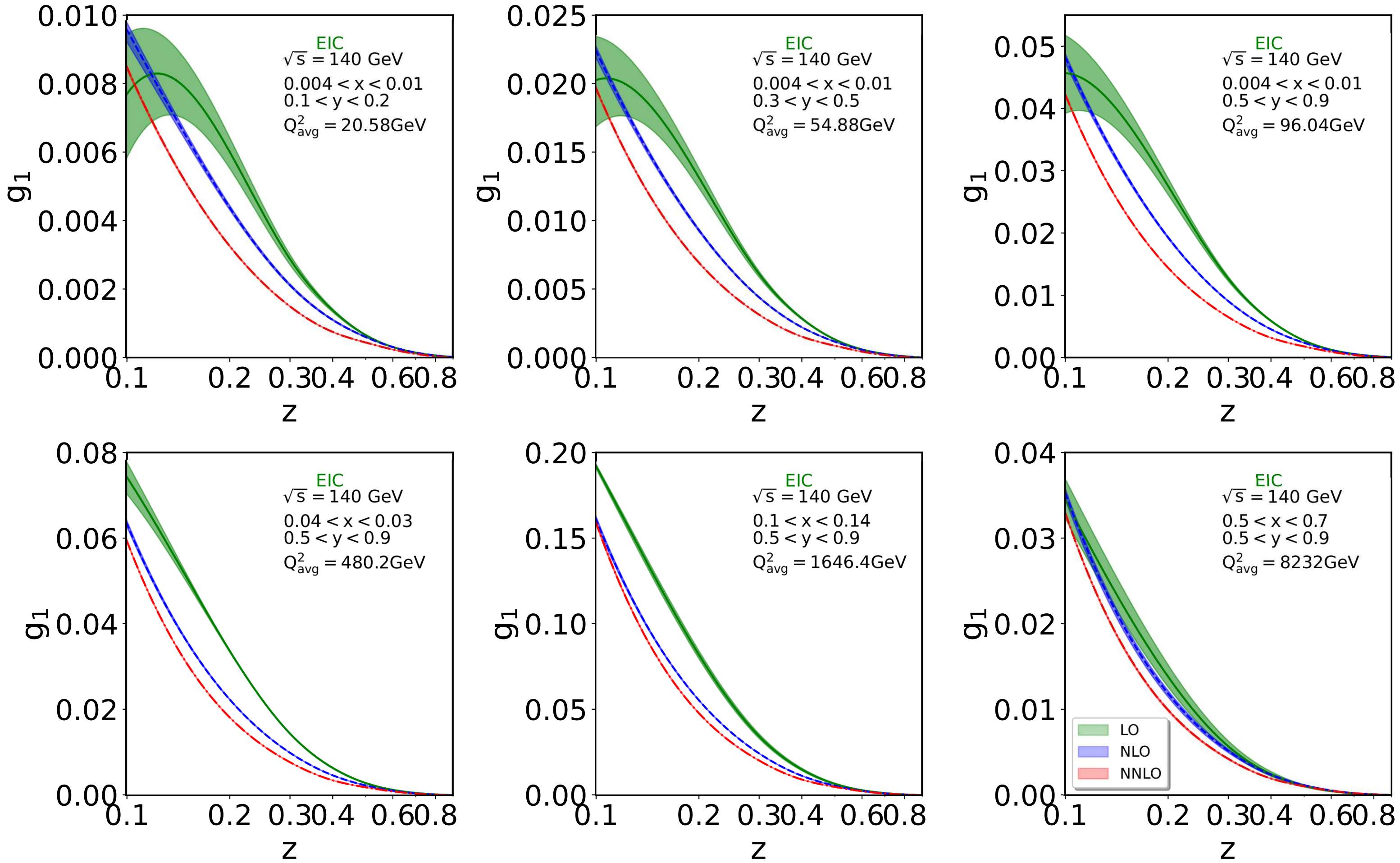

- Scale variation of g_1 as function x for six different values of Q^2; (BDSSV24(N)NLO g_1; NNFF10PIp FFs)

Pion multiplicity

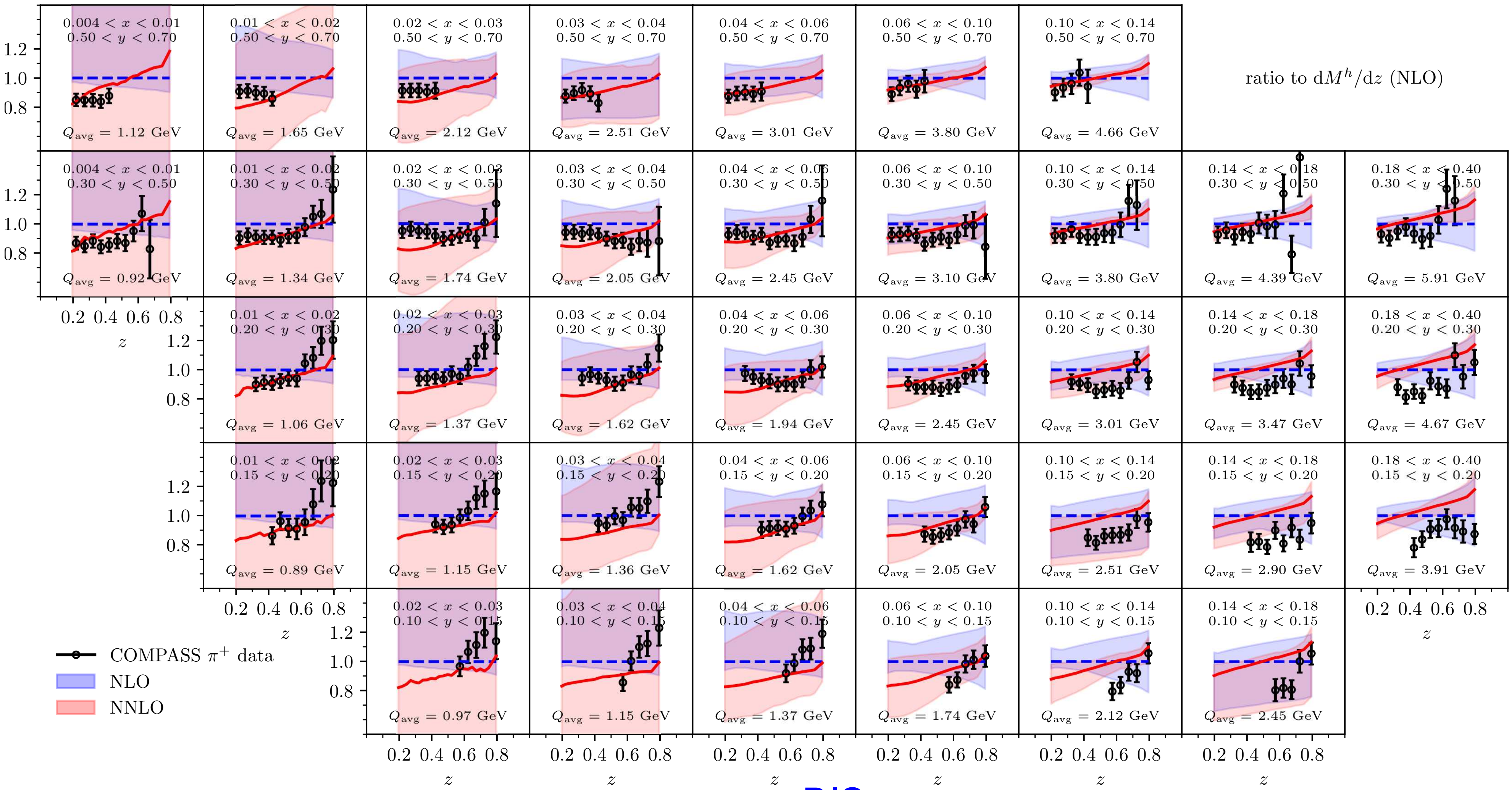

- Pion multiplicity $\frac{dM_{\pi^*}}{dz} = \frac{d^3\sigma^{\pi^+}}{dxdydz} \Big/ \frac{d^3\sigma^{\text{DIS}}}{dxdy}$ compared to COMPASS data taken at $\sqrt{s} = 17.4$ GeV at NLO and NNLO   Bonino, Gehrmann, Stagnitto '24
  - NNPDF31 PDFs; BDSSV22(N)NLO FFs

Polarized SIDIS at COMPASS

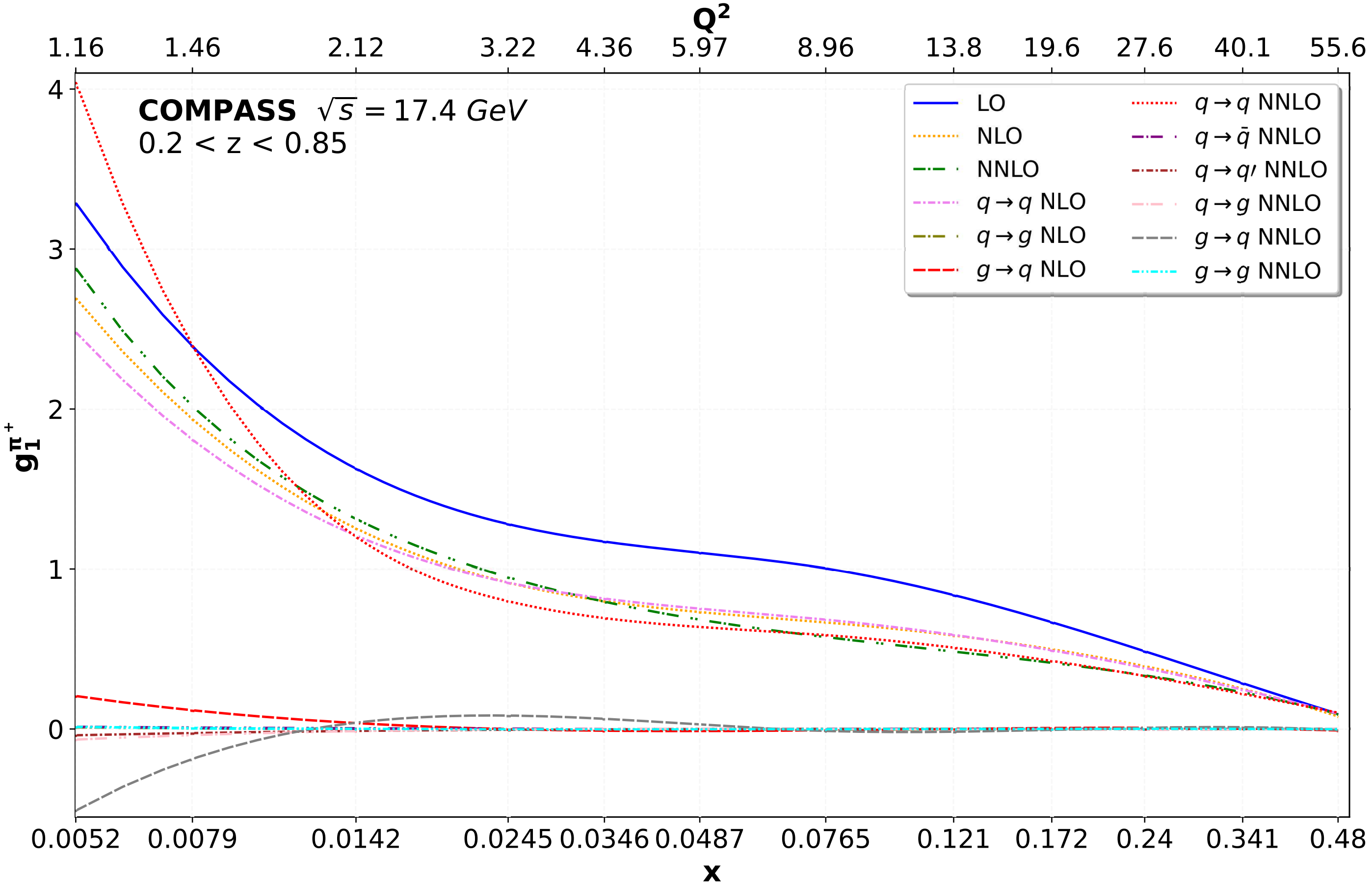

- Contributions from all partonic channels to $g_1^{\pi^+}(x)$ for COMPASS energy $\sqrt{s} = 17.4$ GeV
  - polarized PDFs from MAPPDF10 (Bertone, Chiefa, Nocera '24)
  - FFs from NNFF10 (Bertone, Carrazza, Hartland, Nocera, Rojo '17)

Polarized structure function

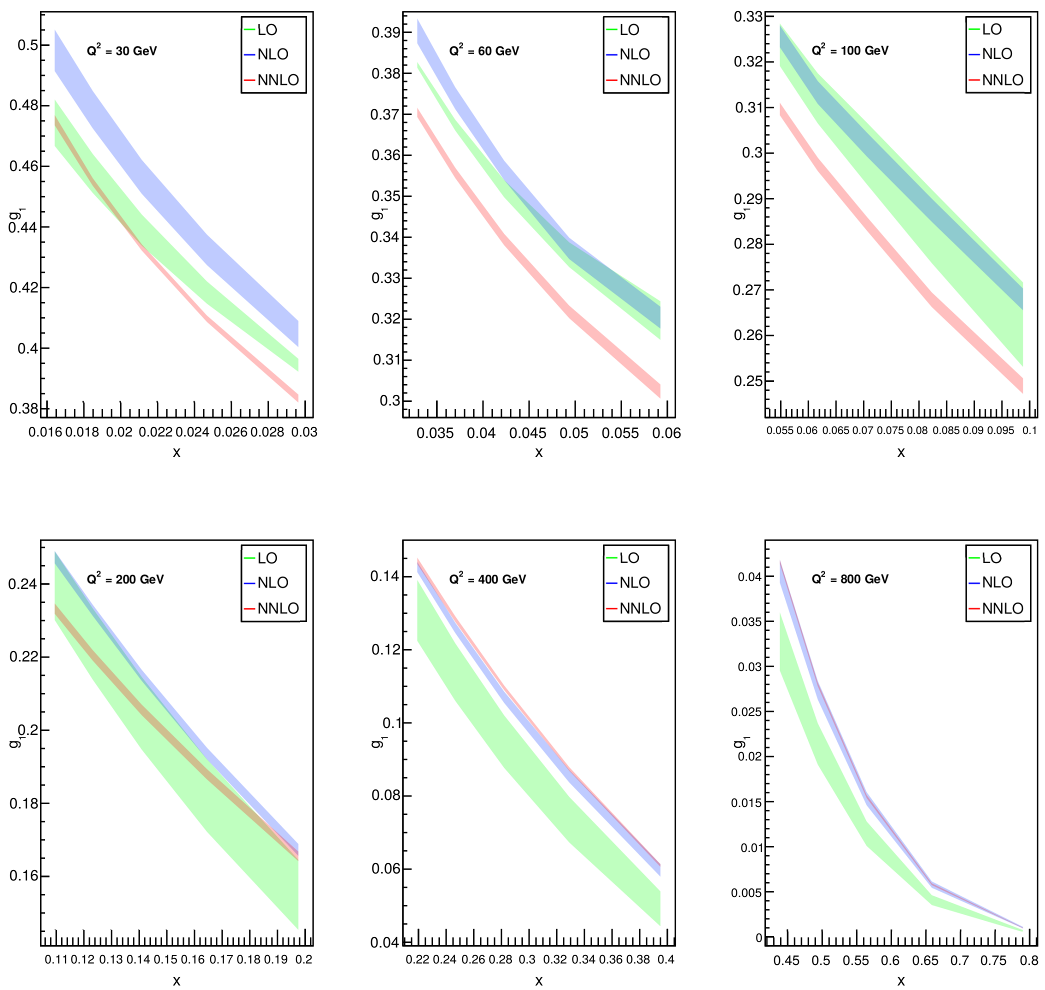

- Scale dependence of $g_1^{\pi^+}(x)$ at various values of Q^2 in 7-point variation of μ_R and μ_F for energy $\sqrt{s} = 45$ GeV
  - polarized PDFs from MAPPDF10 (Bertone, Chiefa, Nocera '24)
  - FFs from MAPFF10 (Abdul Khalek, Bertone, Khoudli, Nocera '22)

Spin asymmetry at COMPASS

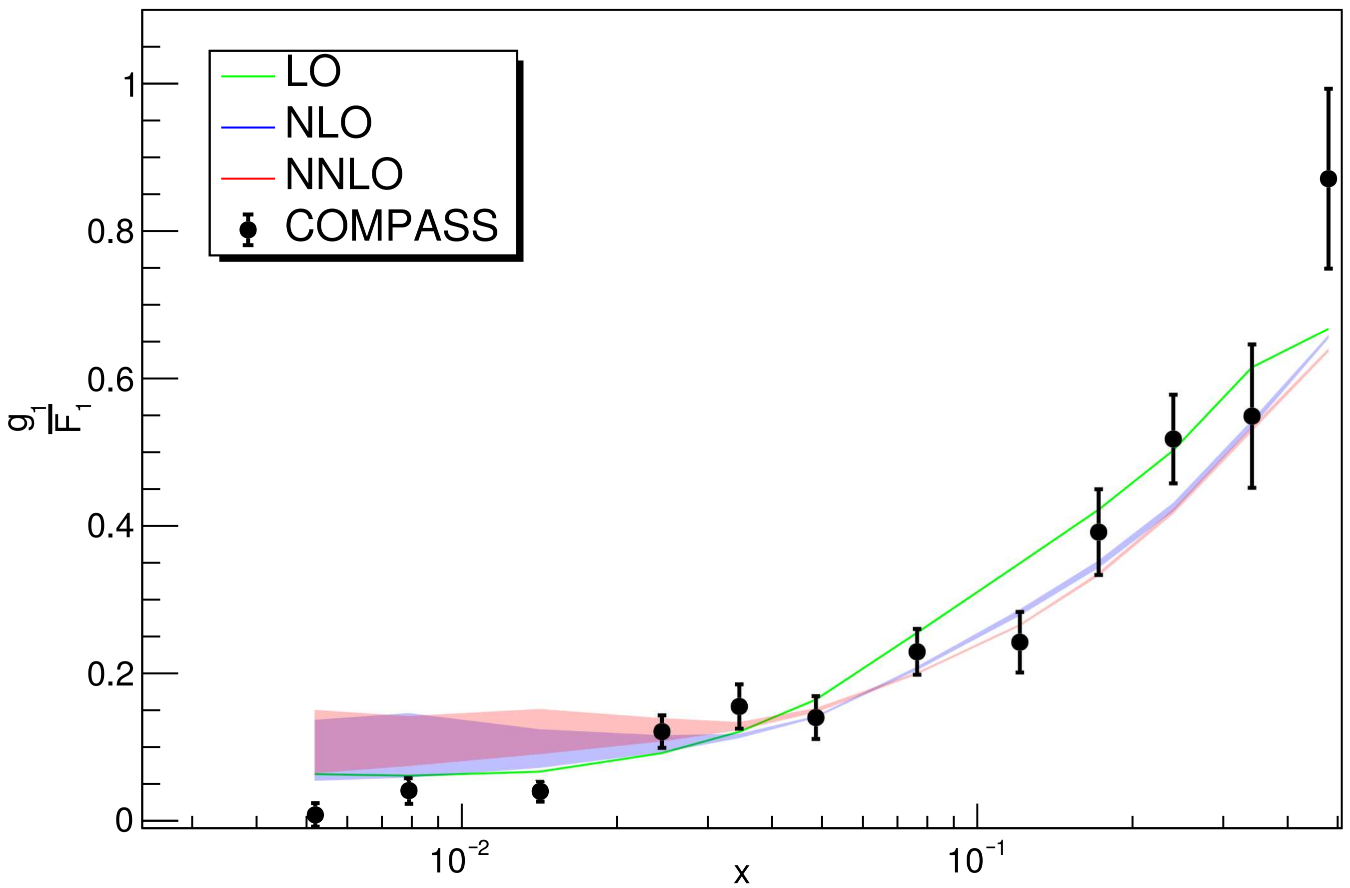

- Ratio of $g_1^{\pi^+}(x)/F_1^{\pi^+}(x)$ for COMPASS energy $\sqrt{s} = 17.4$ GeV with 7-point scale variation
  - polarized PDFs from MAPPDF10 (Bertone, Chiefa, Nocera '24)
  - unpolarized PDFs from NNPDF31
  - FFs from MAPFF10 (Abdul Khalek, Bertone, Khoudli, Nocera '22)

Spin asymmetry at EIC

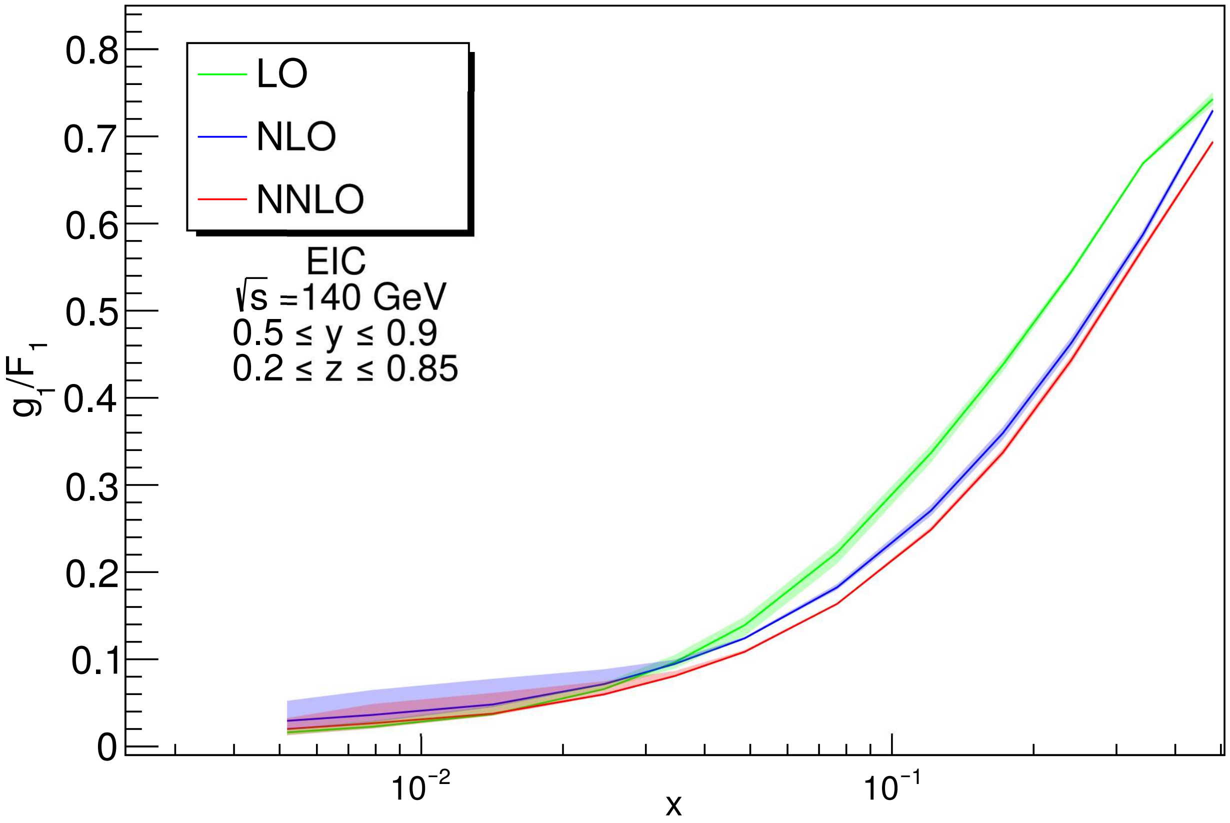

- Asymmetry g_1/F_1 as function of x for EIC at $\sqrt{s} = 140$ GeV
  - polarized PDFs from MAPPDF10 (Bertone, Chiefa, Nocera '24)
  - unpolarized PDFs from NNPDF31
  - FFs from MAPFF10 (Abdul Khalek, Bertone, Khoudli, Nocera '22)

Neutrino-nucleon SIDIS (1)

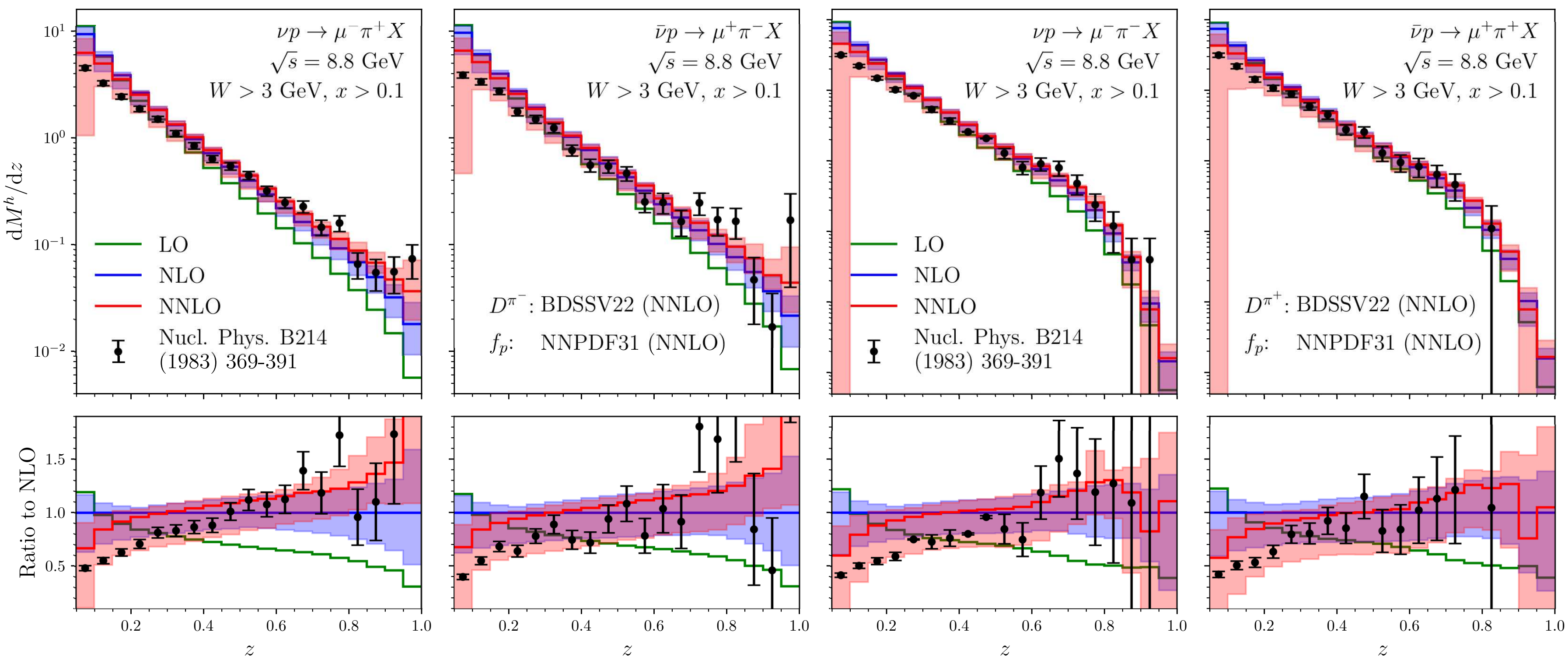

- $\nu(k) + p(P) \to l^+(k') + h(P_h) + X$ with neutrino beam $E_\nu = 39$ GeV
- Pion multiplicity $\frac{dM^{\pi^\pm}}{dz} = \frac{d^3\sigma^{\pi^\pm}}{dxdydz} / \frac{d^3\sigma^{\text{DIS}}}{dxdy}$ compared to data from Aachen-Bonn-CERN-Munich-Oxford (ABCMO) collaboration taken at $\sqrt{s} = 8.8$ GeV at NLO and NNLO   Bonino, Gehrmann, Löchner, Schönwald '25

Neutrino-nucleon SIDIS (2)

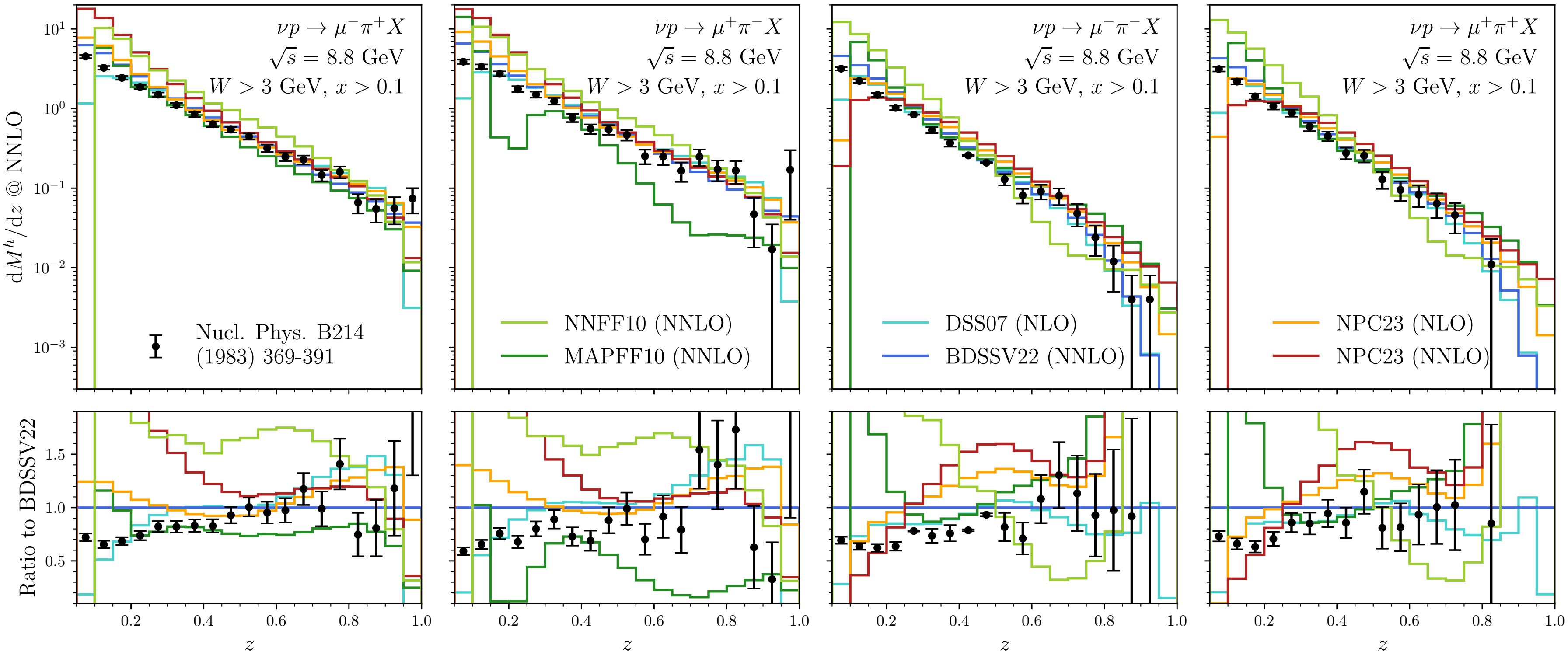

- Comparison of NNLO pion multiplicities $\dfrac{dM^{\pi^\pm}}{dz} = \dfrac{d^3\sigma^{\pi^\pm}}{dxdydz} \Big/ \dfrac{d^3\sigma^{\text{DIS}}}{dxdy}$ computed with different FFs to data Bonino, Gehrmann, Löchner, Schönwald '25
  - ratios with respect to multiplicity computed with BDSSV22NNLO FFs

Summary

- Deep-inelastic scattering
  - Upcoming EIC will probe perturbative QCD in large range of kinematics
  - State-of-the-art detector can aim at experimental precision of $\lesssim 1\%$
- Polarized beams at EIC offer vast opportunities
  - new interest in large class of spin dependent observables
- Precision studies of hadron structure require higher orders in perturbative QCD
  - theoretical predictions at NNLO in QCD nowadays standard
- Furhter improvements for SIDIS
  - joint resummation beyond N^{3}LL accuracy
  - N^{3}LO QCD corrections within reach of current technologies